Applied Mathematics and Mechanics
(English Edition, Vol. 2 No. 6, Dec. 1981)

Published by Techmodern Business
Promotion Centre. Hong Kong

ANALYSIS OF ELLIPSOID COMPRESSED BY TWO AXIAL CONCENTRATED FORCES AT TWO ENDS

Yun Tian-quan 云天铨 , Shao Yong-chang肖永谦
Qiu Chong-guang 邱崇光

(Huazhong Institute of Technology, Wuhan)
(Received on March 20, 1981)

Abstract

Integral equation method and photoelastic experiment are used for the stress analysis of an axial compressive ellipsoid. Let the concentrated forces and the centers of compression, with symmetrical unknown intensive functions $X_1(c)=X_1(-c)$ and $X_2(c)=X_2(-c)$ respectively, be distributed symmetrically to $z=0$ plane along the axis $z(=-c)$ in $[a,\infty)$ and $[-a,-\infty)$ of the elastic space, in addition to a pair of equal and opposite axial forces acting on $z=a$ and $z=-a$. We can reduce the problem of an axial compressive ellipsoid to two coupled Fredholm integral equations of the first kind. Furthermore, numerical calculation is then made. Two photo-elastic models of ellipsoid were analysed by "Freezing and Cutting" method, and the results, in which σ_z is quite nearly to those obtained by integral equation method, had been used in the analysis of the data of compressive rock specimens.

I. Introduction

The three-dimensional axisymmetrical problem of a compressive ellipsoid by two axial concentrated forces is one of the important problems for the strength analysis of rock specimens[1]. However, such problem which seems ever be solved, is trying to be analysed by integral equation method and photoelastic experiment.

As is well-known[2], the integral equation methods often give accurate results more economically than the finite element method for those elastic problems with low surface/volume ratio. However, most of the authors derived their integral equations by means of fictitious elementary loads directly distributed on the actual boundary and the problem was reduced to two-dimensional singular integral equations. Obviously, numerical calculation for such integral equations is laborious.

A simple integral equation method is suggested for this problem, i.e. the method of fictitious elementary loads be distributed along the symmetrical axis but outside the ellipsoid. Such analytic method was suggested and used for several problems by the author[3,4] and the numerical calculation is simpler than other inte-

gral equation methods. Because the integral equations obtained are nonsingular, one-dimensional and the numerical calculation of such integral equations is simple.

In section II the integral equations are derivated. According to the symmetry of the problem, all fictitious loads must be distributed symmetrically to $z=0$ plane. For simplification, the concentrated forces and the centers of compression are most suitable to be the fictitious loads. In order to obtain a nonhomogeneous algebraic equations for the discrete calculation of obtained integral equations,we should put two equal and opposite concentrated forces on two ends of the ellipsoid and thus the two coupled one-dimensional nonsingular Fredholm integral equations can be obtained by satisfying the boundary conditions and the equilibrium equations under these fictitious loads application.

In section III, the integral equations are replaced by their discrete form,i.e., nonhomogeneous algebraic equations, which are $2n$ nonhomogeneous algebraic equations and they can be obtained by satisfying the boundary conditions at n points of the boundary (i.e., zero stresses on the surface of the ellipsoid held for n points of the generator). The fictitious loads, which are continuously distributed in $[a, \infty)$,$[-a, -\infty)$,are replaced by that which are constantly distributed in n ranges. These algebraic equations had been solved by DJS-21 computer for $n=10$ and $n=16$.

Section IV shows the stress analysis by the method of photo-elastic experiment. "Freezing and Cutting" method is used as the analytic method. Two models of ellipsoid with $a/b=1.315$ and 1.5 had been analysed, and the stresses at $z=a/2$ plane and along the z-axis are outlined.

Finally, simple comparison of the results obtained by calculation and experiment is shown in Fig.6.

II. Derivation of the Integral Equations

1. Stresses due to fictitious loads.

The stresses at any point $N(r, \theta, z)$ due to the following loads:

i. Concentrated forces and centers of compression with symmetrical unknown intensive function $X_1(c)=X_1(-c)$and $X_2(c)=X_2(-c)$ respectively are distributed symmetrically to $z=0$ plane along the $z(=-c)$ axis in $[a, \infty)$ and $[-a, -\infty)$ of the elastic space;

ii. A pair of equal and opposite acial force axting on $z=a$ and $z=-a$ along the z-axis of the elastic space is:

$$\sigma_r=K\int_a^{\infty}((1-2\nu)((z+c)R_{1c}^{-3}-(z-c)R_{2c}^{-3})-3r^2((z+c)R_{1c}^{-5}-(z-c)R_{2c}^{-5}))X_1(c)\,dc+K_1\int_a^{\infty}((r^2-0.5(z+c)^2)R_{1c}^{-5}$$

$$
\begin{aligned}
&+(r^2-0.5(z-c)^2)R_{2c}^{-5})X_2(c)dc+KP((1-2\nu)((z+a)R_1^{-3}\\
&-(z-a)R_2^{-3})-3r^2((z+a)R_1^{-5}-(z-a)R_2^{-5}))\\
\sigma_\theta=&K\int_a^\infty(1-2\nu)((z+c)R_{1c}^{-3}-(z-c)R_{2c}^{-3})X_1(c)dc-0.5K_1\\
&\cdot\int_a^\infty(R_{1c}^{-3}+R_{2c}^{-3})X_2(c)dc+KP(1-2\nu)((z+a)R_1^{-3}-(z-a)R_2^{-3})\\
\sigma_z=&-K\int_a^\infty((1-2\nu)((z+c)R_{1c}^{-3}-(z-c)R_{2c}^{-3})+3((z+c)^3R_{1c}^{-5}\\
&-(z-c)^3R_{2c}^{-5}))X_1(c)dc+K_1\int_a^\infty(((z+c)^2-0.5r^2)R_{1c}^{-5}\\
&+((z-c)^2-0.5r^2)R_{2c}^{-5})X_2(c)dc-KP((1-2\nu)((z+a)R_1^{-3}\\
&(z-a)R_2^{-3})+3((z+a)^3R_1^{-5}-(z-a)^3R_2^{-5}))\\
\tau_{rz}=&-K_r\int_a^\infty((1-2\nu)(R_{1c}^{-3}-R_{2c}^{-3})+3((z+c)^2R_{1c}^{-5}\\
&-(z-c)^2R_{2c}^{-5}))X_1(c)dc+1.5K_1r\int_a^\infty((z+c)R_{1c}^{-5}\\
&+(z-c)R_{2c}^{-5})X_2(c)dc-KPr((1-2\nu)(R_1^{-3}-R_2^{-3})+3((z+a)^2R_1^{-5}\\
&-(z-a)^2R_2^{-5}))
\end{aligned}
\tag{2.1}
$$

where:

$$
\begin{aligned}
&R_{1c}=(r^2+(z+c)^2)^{1/2}\\
&R_{2c}=(r^2+(z-c)^2)^{1/2}\\
&R_1=(r^2+(z+a)^2)^{1/2}\\
&R_2=(r^2+(z-a)^2)^{1/2}\\
&K=(8\pi(1-\nu))^{-1}\\
&K_1=\text{const.}\\
&P=\text{const.}\\
&\nu\ \text{Poisson's ratio}\\
&a\ \text{half longest distance of ellipsoid.}\\
&c\ \text{depth of the fictitious loads at } z=c\ .\\
&X_1(c),\ X_2(c)\ \text{unknown intensive functions of concentrated forces and centers of compression.}\\
&r,\ \theta,\ z\ \text{cylindrical coordinates.}
\end{aligned}
\tag{2.2}
$$

2. Stress boundary conditions.

According to the fact that stresses on the surface of the ellipsoid with generating function $\left(\frac{r}{b}\right)^2+\left(\frac{z}{a}\right)^2=1$ must equal to zero, from the equilibrium equations, we have the following equations held at boundary:

$$\sigma_r=\tau_{rz}\cdot dr/dz \tag{2.3}$$

$$\tau_{rz}=\sigma_z\cdot dr/dz \tag{2.4}$$

Substituting (2.1) into (2.3) and (2.4), we have

$$A_1X_1+B_1X_2=F_1 \tag{2.5}$$

$$A_2X_1+B_2X_2=F_2 \tag{2.6}$$

where A_1, A_2, B_1, B_2 are kernel operators of the integral equations. F_1, F_2 are

known functions.

$$
\left.\begin{aligned}
A_1 &= A_1(z,c) = K((1-2\nu)((z+c)R_{ac}^{-3} - (z-c)R_{bc}^{-3}) \\
&\quad -3b^2(1-(z/a)^2)((z+c)R_{ac}^{-5} - (z-c)R_{bc}^{-5}) + (dr/dz)b(1 \\
&\quad -(z/a)^2)^{1/2}((1-2\nu)(R_{ac}^{-3} - R_{bc}^{-3}) + 3((z+c)^2 R_{ac}^{-5} - (z-c)^2 R_{bc}^{-5})) \\
A_2 &= A_2(z,c) = -K(b(1-(z/a)^2)^{1/2}((1-2\nu)(R_{ac}^{-3} - R_{bc}^{-3}) \\
&\quad +3((z+c)^2 R_{ac}^{-5} - (z-c)^2 R_{bc}^{-5})) - (dr/dz)((1-2\nu)((z+c)R_{ac}^{-3} \\
&\quad -(z-c)R_{bc}^{-3}) + 3((z+c)^3 R_{ac}^{-5} - (z-c)^3 R_{bc}^{-5}))) \\
B_1 &= B_1(z,c) = K_1((b^2(1-(z/a)^2) - 0.5(z+c)^2)R_{ac}^{-5} + (b^2(1-(z/a)^2) \\
&\quad -0.5(z-c)^2)R_{bc}^{-5} - 1.5(b(1-(z/a)^2)^{1/2}((z+c)R_{ac}^{-5} \\
&\quad +(z-c)R_{bc}^{-5}) \cdot (dr/dz))) \\
B_2 &= B_2(z,c) = K_1(1.5b(1-(z/a)^2)^{1/2}((z+c)R_{ac}^{-5} + (z-c)R_{bc}^{-5}) \\
&\quad -(dr/dz)(((z+c)^2 - 0.5b^2(1-(z/a)^2))R_{ac}^{-5} + ((z-c)^2 \\
&\quad -0.5b^2(1-(z/a)^2))R_{bc}^{-5})) \\
F_1 &= F_1(z) = -KP((1-2\nu)((z+a)R_a^{-3} - (z-a)R_b^{-3}) \\
&\quad -3b^2(1-(z/a)^2)((z+a)R_a^{-5} - (z-a)R_b^{-5}) + (dr/dz)b(1 \\
&\quad -(z/a)^2)^{1/2}((1-2\nu)(R_a^{-3} - R_b^{-3}) + 3((z+a)^2 R_a^{-5} - (z-a)^2 R_b^{-5}))) \\
F_2 &= F_2(z) = KP(b(1-(z/a)^2)^{1/2}((1-2\nu)(R_a^{-3} - R_b^{-3}) + 3((z+a)^2 R_a^{-5} \\
&\quad -(z-a)^2 R_b^{-5})) - (dr/dz)((1-2\nu)((z+a)R_a^{-3} - (z-a)R_b^{-3}) \\
&\quad +3((z+a)^3 R_a^{-5} - (z-a)^3 R_b^{-5})))
\end{aligned}\right\} \qquad (2.7)
$$

where

$$
\left.\begin{aligned}
dr/dz &= -b^2 z/a^2 r = -(b/a^2)z(1-(z/a)^2)^{-1/2} \\
R_{ac} &= (b^2(1-(z/a)^2) + (z+c)^2)^{1/2} \\
R_{bc} &= (b^2(1-(z/a)^2) + (z-c)^2)^{1/2} \\
R_a &= (b^2(1-(z/a)^2) + (z+a)^2)^{1/2} \\
R_b &= (b^2(1-(z/a)^2) + (z-a)^2)^{1/2}
\end{aligned}\right\} \qquad (2.8)
$$

Thus, our problem is reduced to two coupled Fredholm integral equations (2.5), (2.6) and the equilibrium equations (2.9), (2.10). The latter two equations are utilized to determine the relationship between applied load Q and constants P, K_1 .

$$
\int_{s_1} \sigma_z ds = Q \qquad (2.9)
$$

$$
\int_{s_2} \sigma_\theta ds = 0 \qquad (2.10)
$$

Where s_1, s_2 denote the sectional areas cut by $z=0$ plane and $y=0$ plane respectively.

Once the solutions X_1, X_2, K_1 and P have been obtained from (2.5), (2.6), (2.9) and (2.10), we can calculate the stresses from (2.1).

III. Discrete Calculation of the Integral Equations

A common simple numerical treatment of integral equations (2.5) and (2.6) is to replace itself by its discrete form, i.e., let the boundary conditions (2.3) and (2.4) be satisfied at n points of the generator $\left(\frac{r}{b}\right)^2+\left(\frac{z}{a}\right)^2=1$ (i.e., zero stresses on the surface of the ellipsoid held for n points of the generator); and the fictitious loads which are continuously distributed in $[a, \infty),[-a, -\infty)$, are replaced by that which are constantly distributed in n ranges; then we can rewrite (2.5), (2.6) as follows:

$$\left.\begin{aligned}\sum_{j=1}^{n}A_{1ij}X_{1j}+\sum_{j=1}^{n}B_{1ij}X_{2j}=F_{1i}\\ \sum_{j=1}^{n}A_{2ij}X_{1j}+\sum_{j=1}^{n}B_{2ij}X_{2j}=F_{2i}\end{aligned}\right\} i=1, 2, \cdots, n. \tag{3.1}$$

Where

$$\left.\begin{aligned}&X_{tj}=X_t(c_j),\ F_{ti}=F_t(z_i)\\ &A_{tij}=\int_{ja}^{(j+1)a}A_t(z_i, c)dc\\ &B_{tij}=\int_{ja}^{(j+1)a}B_t(z_i, c)dc\end{aligned}\right\}\begin{aligned}&t=1, 2;\\ &i, j=1, 2, \cdots, n.\end{aligned} \tag{3.2}$$

Similarly, (2.9), (2.10) can be rewritten as:

$$2\pi(b/m)^2\sum_{i=1}^{m}i\sigma_z(ib/m, 0)=Q \tag{3.3}$$

$$ab/(mL)\sum_{i=1}^{m}\sum_{t=1}^{L}\sigma_r(ib/m, ta/L)=0 \tag{3.4}$$

Where $\sigma_z(r, z)$ and $\sigma_r(r, z)$ are shown in (2.1); but if $t>L\sqrt{1-(i/m)^2}$, let $\sigma_r(ib/m, ta/L)=0$.

Solve (3.1)-(3.4), we can obtain X_1, X_2, P and K_1 . Then the stresses can be obtained from (2.1).

The example used for the ellipsoidic model possesses: half longest distance of the ellipsoid $a=2.2875$cm, half shortest distance of the ellipsoid $b=1.525$cm, $a/b=1.5$; Poisson's ratio $\nu=0.45$; applied load $Q=23.08$kg. We use DLS-21 computer for calculation; the integrals are approximated by Romberg formula and trapezoid formula. These cases of $n=10$ and $n=16$ had been calculated, and the results obtained are shown in Fig. 6.

IV. Photoelastic Stress Analysis of Ellipsoid under Concentrated Loads along the Major Axis

(1) Analytic considerations.

In order to determine the distribution of the stresses in ellipsoid, two models of ellipsoids with $a/b=1.315$ and 1.5 were investigated by frozen method used in three-dimensional photoelasticity.

According to the fact that the problem of ellipsoid under axial forces is axisymmetrical and thus the stress state at any point is independent of θ, all the stress components σ_r, σ_θ, σ_z, τ_{rz} can be determined from two mutually perpendicular slices, i.e., one of them included the axis of symmetry and the other was cut by two adjoining planes parallel to equatorial plane (a horizontal slice). These slices are shown in Fig. 1.

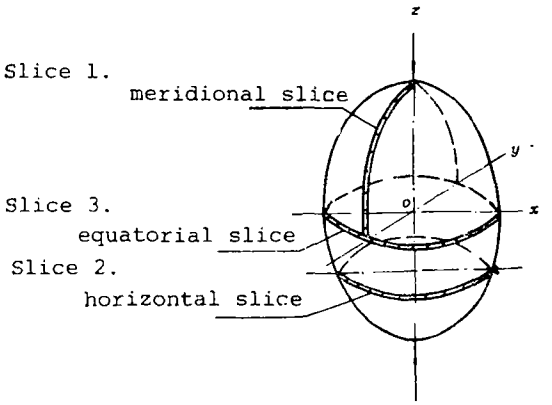

Fig.1. Location of the slices

According to the stress-optical law[5,6], the observed data of an incident ray running through the meridional and horizontal slices normally yield the differences of the secondary principal stresses $(p'-q')_\theta$, $(p'-q')_z$ and the directional angle φ_θ of these stresses, i.e., we have:

$$\left.\begin{aligned}
&\sigma_r-\sigma_z=(p'-q')_\theta\cos 2\varphi_\theta=n_\theta F_\theta\cos 2\varphi_\theta\\
&\tau_{rz}=\frac{1}{2}(p'-q')_\theta\sin 2\varphi_\theta=\frac{1}{2}n_\theta F_\theta\sin 2\varphi_\theta\\
&\sigma_\theta-\sigma_r=(p'-q')_z=n_z F_z
\end{aligned}\right\}\qquad(4.1)$$

where n_θ, n_z denote the fringe orders associated with the normal incidence patterns; F_θ, F_z denote the fringe values of the slices respectively; the subscripts θ, z denote the directions, in which the light propagates through the slices.

Although the equations in formula (4.1) are independent of each other, however, there are four unknowns, i.e. σ_r, σ_θ, σ_z and τ_{rz} so that the individual normal stresses could not be determined directly. For the sake of separating the normal stresses, equations of equilibrium must be used as a supplementary. The equilibrium equations of the axisymmetrical problem in the case of absence of body forces are:

$$\left.\begin{aligned}\frac{\partial\sigma_r}{\partial r}+\frac{\partial\tau_{rz}}{\partial z}+\frac{\sigma_r-\sigma_\theta}{r}=0\\ \frac{\partial\tau_{rz}}{\partial r}+\frac{\partial\sigma_z}{\partial z}+\frac{\tau_{rz}}{r}=0\end{aligned}\right\} \tag{4.2}$$

If we integrate the first equation in formula (4.2) with respect to r, we have:

$$(\sigma_r)_i=(\sigma_r)_0-\int_0^i\frac{\partial\tau_{rz}}{\partial z}dr-\int_0^i\frac{\sigma_r-\sigma_\theta}{r}dr$$

or in finite difference form,

$$(\sigma_r)_i=(\sigma_r)_0-\sum_0^i\frac{\Delta\tau_{rz}}{\Delta z}\Delta r-\sum_0^i\frac{\sigma_r-\sigma_\theta}{r}\Delta r \tag{4.3}$$

where $(\sigma_r)_0$ denotes the σ_r at the starting point o, and $(\sigma_r)_0$ is known; $(\sigma_r)_i$ denotes the normal stress at point i along the integral path. The first sum of the right part can be computed from the photoelastic data of the meridional slice while the second sum can be obtained by horizontal slice. If the horizontal slice is not to be cut, the values of the $(\sigma_r-\sigma_\theta)$ can be evaluated by observing the meridional slice under oblique incidence. From these two sums the stress σ_r can be obtained. After that the σ_θ, σ_z may be found by using the first and the third of eq. (4.1). Thus, from the observed photoelastic data of normal incidence of two mutually perpendicular slices together with the integrating of the differential equation of equilibrium, one can obtain the solution of the problem, i.e. four stress components σ_r, σ_z, σ_θ, τ_{rz}

The stress components at the points of the axis of symmetry can be calculated by integrating (4.2) with a known starting point $(\sigma_z)_0$ obtained from the above calculation. In this case we have:

$$(\sigma_z)_i=(\sigma_z)_0-\int_0^i\frac{\partial\tau_{rz}}{\partial r}dz-\int_0^i\frac{\tau_{rz}}{r}dz=(\sigma_z)_0-2\int_0^i\frac{\tau_{rz}}{r}dz$$

or in finite difference form:

$$(\sigma_z)_i=(\sigma_z)_0-2\sum_0^i\frac{\Delta\tau_{rz}}{\Delta r}\Delta z=(\sigma_z)_0-2\sum_0^i\frac{\tau_{rz}}{r}\Delta z \tag{4.4}$$

In the procedure of separating the normal stresses, the path of integration is taken along the A_1o_1 at first and then along o_1o, and finally from point A to o (Fig.2). Thus, the accuracy of the results can be checked from the fact that for the same point the values of stress σ_z obtained by the integrations with different paths must be equal to each other. Because the line of integration oA being the axis of symmetry and it is also a trajectory of principal stress, so it is con-

venient to separate the principal stresses by integrating the Lamê-Maxwell equations:

$$\left.\begin{aligned} p_i &= p_0 - \int_0^i (p-q)\frac{d\theta}{dy}ds_1 \\ q_i &= q_0 - \int_0^i (p-q)\frac{d\theta}{dx}ds_2 \end{aligned}\right\} \qquad (4.5)$$

or

$$q_i = q_0 - \frac{1}{\Delta x}\sum_0^i (p-q)\Delta\theta\Delta y$$

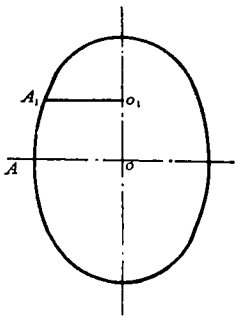

Fig.2. Integral path

Where p, q represent the principal stresses or secondary principal stresses; $\frac{d\theta}{dy}$ represents the variational ratio of the angle included between tangent of the trajectory and horizontal axis with respect to y ; Δy denotes the distance from horizontal axis to the closing isoclinic; Δx denotes finite intervals along x , i.e. Δs or s .

(2) Results of the photoelastic test and the checking of its accuracy.

The results of photoelastic test of two ellipsoids are given below. Fig.3a shows the isochromatic fringe pattern of the integral ellipsoid with $a/b=1.315$,while isochromatic fringe patterns of its meridional and horizontal slices are illustrated in Figs. 3b and 3c respectively. Figs. 4a and 4b show the isochromatic fringe patterns of the meridional and horizontal slices of the ellipsoid with $a/b=1.5$ respectively. The curves of the normal stresses along the considered sections of the two ellipsoids are plotted in Figs. 5 and 6.

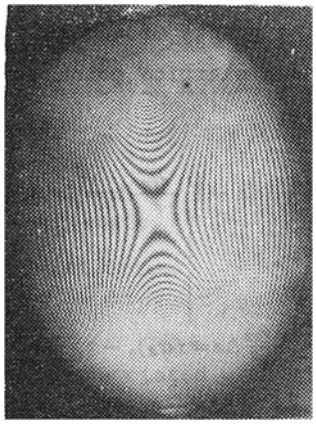

Fig. 3a. Isochromatic fringe pattern of the integral ellipsoid with $(a/b=1.315)$

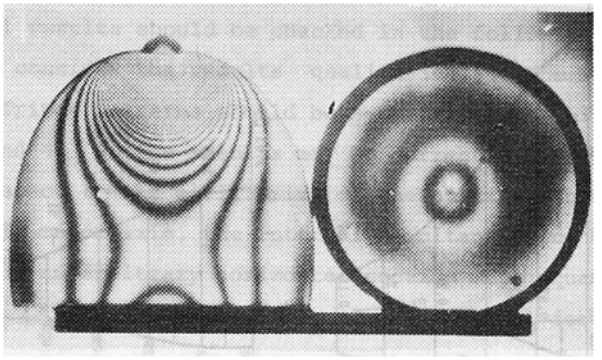

Fig.3b. *Isochromatic fringe pattern of the meridional slice cut from this ellipsoid*

Fig.3c. *Isochromatic fringe pattern of the horizontal slice cut from this ellipsoid*

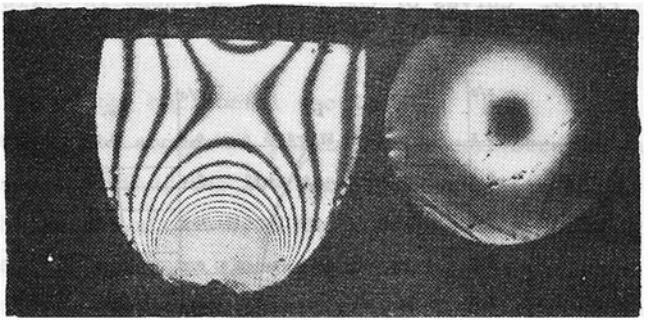

4a *4b*

Fig.4a. *Isochromatic fringe pattern of the meridional slice cut from the ellipsoid with* (a/b=1.5)

Fig.4b. *Isochromatic fringe pattern of the horizontal slice cut from the same ellipsoid*

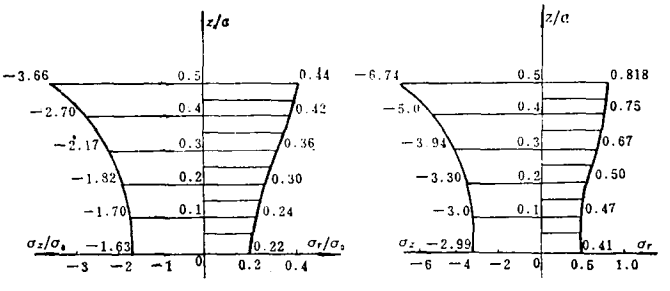

a) Curves of the ratio $\sigma_z/\sigma_0, \sigma_r/\sigma_0$, *where* $\sigma_0=\frac{Q}{A}=1.836$ (kg/cm²); *is the area of the equatorial plane*

b) Curves of the σ_z, σ_r (kg/cm²) *on the axis of symmetry* oz

Fig.5. *Curves of the normal stresses in ellipsoid with* (a/b=1.315)

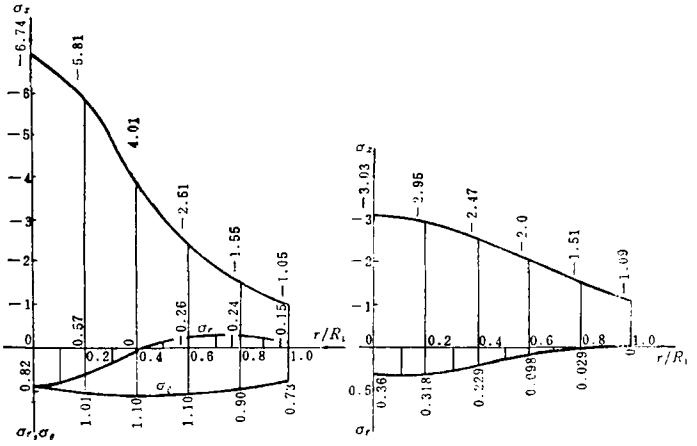

c) Curves of the $\sigma_z, \sigma_r, \sigma_\theta$ along the section o_1R_1 (A_1o_1)

d) Curves of the $\sigma_z, \sigma_r, \sigma_\theta$ along the section Ao

Fig.5. Curves of the normal stresses in ellipsoid with (b/a=1.315)

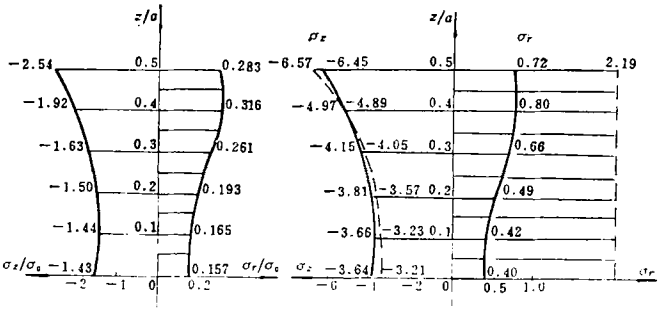

a) Curves of the ratio σ_z/σ_0 and σ_r/σ_0 along the axis of symmetry oz σ_0=2.54kg/cm².

b) Curves of the σ_r, σ_z(kg/cm²) along the axis of symmetry oz

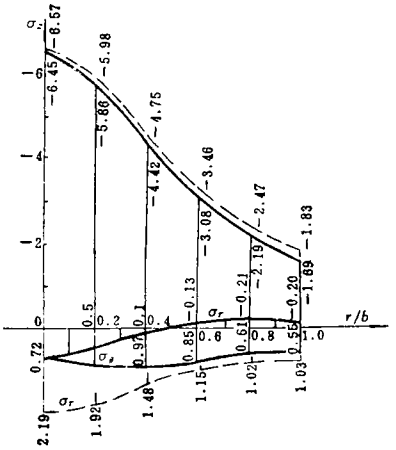

c) Curves of the $\sigma_r, \sigma_\theta, \sigma_z$ along the radius of $z=\frac{a}{2}$ plane

Fig.6. Curves of the normal stresses in the ellipsoid with (a/b=1.5)

Check the accuracy of the experimental results.

The experimental results should be checked in the following way:

Firstly, let us consider the results qualitatively. The models have axis of symmetry and their fringe patterns should be symmetrical to this axis too. This is true in Figs.3 and 4. So the results may be corrected. Secondly, the check may be done with respect to the equilibrium of the statical forces. For an ellipsoid loaded along its major axis, the internal resultant force acting over the equatorial section or an arbitrary horizontal section must equal to the applied external load. Let Q' and Q be the internal and external forces respectively. We have:

$$Q' \doteq \int_0^R 2\pi r(\sigma_z)_r dr \tag{4.6}$$

or

$$Q' = \frac{2\pi R}{\beta^2 n} \sum_{i=1}^{n} \bar{r}_i \, \bar{\sigma}_{z(i)} = \frac{2\pi R}{\beta^2 n} \left[\frac{1}{4} (r_1 \sigma_{z(0)} + 3r_1 \sigma_{z(1)} + 2r_n \sigma_{z(n)}) + \sum_{i=2}^{n-1} r_i \sigma_{z(i)} \right] \tag{4.7}$$

where

R ——— the radius of the horizontal section;

r_i, $\sigma_{z(i)}$ ——— radii of the segmental points and normal stresses at these points;

$\bar{r}_i$, $\bar{\sigma}_{z(i)}$ ——— average radii of the two neighbouring points and average values of the normal stresses at the corresponding points repectively;

n ——— number of the segments along the section;

β ——— magnification of the fringe pattern.

Substituting the value of $\sigma_{z(i)}$ given in Fig.5 into formula (4.7), we obtain the resultant force over the horizontal area at $z=\frac{a}{2}$ of the ellipsoid $(a/b=1.315)$ $Q=23.08\text{kg}$ However, the applied load $Q'=23.45\text{kg}$, so that the error of the statical forces in equilibrium is given:

$$\varepsilon = \frac{Q'-Q}{Q} \times 100\% = \frac{23.45-23.08}{23.08} \times 100\% = 1.5\%$$

In a similar way, we have calculated the error $\varepsilon=0.43\%$ for another ellipsoid $(a/b=1.5)$.

Finally, the accuracy of the results may be tested approximately by comparing various normal stresses, obtained from different paths, at the same point. For ellipsoid with $(a/b=1.315)$ at first, we integrated equation (4.3) from point A , which is passing through point o_1 to point o (Fig.2) and obtained $\sigma_z=-2.993\text{kg/cm}^2$ $\sigma_r=0.407\text{kg/cm}^2$. Then the path of integration was taken from point A to o and we obtained $\sigma_z=-3.026\,\text{kg/cm}^2$, $\sigma_r=0.36\,\text{kg/cm}^2$. The differences between these stresses are very small.

Fig.6 shows the results of normal stresses obtained by the calculation of the discrete form of the integral equations (dotted lines) and by the experiment of photoelasticity (continuous lines). We can see the results of σ_z obtained by

these two methods are quite near to each other; but σ_r are not so good. This may be caused by the rough calculation, especially in (3.4). If the elements are cut smaller (i.e., n,m,l larger), the results may be better.

References

1. *Broch, E. and Franklin, J. A., The point-load strength test, International Journal of Rock Mechanics and Mining Science, 9, 6, 1972.*
2. *Banerjee, P. K., Integral equation method for analysis of piece-wise non-homogeneous three-dimensional elastic solids of arbitrary shape, Int. J. Mech. Sci., 18, 293, (1976).*
3. *Yun, T. Q., A simple integral equation method for three-dimensional problems of cylinder embedded in a half-space, Acta Mechanica Solida Sinica, 1, 2, (1980). (in Chinese)*
4. *Yun. T. Q., An iteration method for integral equations arising from axisymmetric loading problems, Appl. Math. & Mech., 1, 1, (1980). 121-131.*
5. *Frocht, M. M., Photoelasticity 11, (1948).*
6. *Kuske, A., Photoelastic Stress Analysis, (1973).*